European Heart Journal – Cardiovascular Imaging (2015) **16**, 1137–1147
doi:10.1093/ehjci/jev058

The influence of frame rate on two-dimensional speckle-tracking strain measurements: a study on silico-simulated models and images recorded in patients

Assami Rösner[1]*, Daniel Barbosa[2,3], Erling Aarsæther[4], Didrik Kjønås[1], Henrik Schirmer[1,4], and Jan D'hooge[2]

[1]Division of Cardiothoracic and Respiratory Medicine, Department of Cardiology, University Hospital of Northern Norway, 9038 Tromsø, Norway; [2]Department of Cardiovascular Sciences, KU Leuven, Leuven, Belgium; [3]Life and Health Sciences Research Institute, University of Minho, Minho, Portugal; and [4]Department of Clinical Medicine, Arctic University of Norway, Tromsø, Norway

Received 3 November 2014; accepted after revision 18 February 2015; online publish-ahead-of-print 9 March 2015

Aims Ultrasound-derived myocardial strain can render valuable diagnostic and prognostic information. However, acquisition settings can have an important impact on the measurements. Frame rate (i.e. temporal resolution) seems to be of particular importance. The aim of this study was to find the optimal range of frame rates needed for most accurate and reproducible 2D strain measurements using a 2D speckle-tracking software package.

Methods and results Synthetic two dimensional (2D) ultrasound grey-scale images of the left ventricle (LV) were generated in which the strain in longitudinal, circumferential, and radial direction were precisely known from the underlying kinematic LV model. Four different models were generated at frame rates between 20 and 110 Hz. The resulting images were repeatedly analysed. Results of the synthetic data were validated in 66 patients, where long- and short-axis recordings at different frame rates were analysed. In simulated data, accurate strain estimates could be achieved at >30 frames per cycle (FpC) for longitudinal and circumferential strains. Lower FpC underestimated strain systematically. Radial strain estimates were less accurate and less reproducible. Patient strain displayed the same plateaus as in the synthetic models. Higher noise and the presence of artefacts in patient data were followed by higher measurement variability.

Conclusion Standard machine settings with a FR of 50–60 Hz allow correct assessment of peak global longitudinal and circumferential strain. Correct definition of the region of interest within the myocardium as well as the reduction of noise and artefacts seem to be of highest importance for accurate 2D strain estimation.

Keywords Strain imaging • Frame rate • Imaging quality • Simulated model

Introduction

Reproducible and accurate measurements expressing left-ventricular (LV) function have important impact on optimal clinical management of patients in cardiology. The incremental value of regional and global measures of myocardial deformation by strain and strain rate (SR) have been shown in many clinical studies addressing a high variety of cardiac diseases.[1–7] Two-dimensional (2D) speckle-tracking echocardiography (STE) is based on frame-by-frame tracking of echo-dense speckles within the myocardium and subsequent measurement of regional myocardial deformation.[8,9] STE-derived global longitudinal strain (GLS) and global circumferential strain (GCS) are simple deformation parameters and close to routine clinical application. The optimal acquisition rate [i.e. number of frames per second in relation to heart rate (FRpHR) or cycle length (FpC)] seems to have an important impact on accuracy of strain and SR measurements.[10] Studies on tissue velocity imaging (TVI)-derived strain concluded that an optimal frame rate for TVI-based strain measurements would be at least 100 Hz.[11–13] For 2D speckle-tracking-derived strain, most clinical studies have used a standard setting of

* Corresponding author. Tel: +47 77627347; Fax: +47 77628298, Email: assami.rosner@unn.no

40–70 frames per second.[14] However, it is not known to which extent lower or higher frame rates might influence the measured 2D strain values. While clinical studies usually refer to the acquisition rate as frames per second, the biomedical engineering studies clearly indicate that tracking quality depends on the amount of inter-frame displacement/deformation, which depends on the combination of the FR and the HR. Thus FpC is intrinsically connected with the overall tracking quality.[10] In the present study, we mimicked different FR using a 2D simulation framework based on a kinematic left-ventricular model and a physical-based ultrasound image simulator. As such, synthetic ultrasound images were generated with reference motion and strain curves. The aim of the study was to explore the influence of FpC on accuracy, precision, and reproducibility of strain measurements. In addition, we investigated the influence of endo-, myo-, and epicardial ROI position on the accuracy and reproducibility of the measured strain values. The influence of FR on the strain assessment was also studied in real patient data to verify whether the key findings of the *in-silico* experiments were reproducible in clinical data.

Methods

Generation of synthetic image data

A simplified LV kinematic model was used to generate realistic cardiac deformation patterns. The underlying kinematical model was based on the definition of mathematical expressions for the displacement field within a truncated ellipsoid, controlled by different parameters such as LV-torsion, fibre-orientation, or ejection fraction (EF).[15,16] As illustrated in *Figure 1*, the model enables generating 3D ellipsoidal myocardial shapes that present realistic (local) motion/deformation patterns for differing global functional status of the heart. Four different settings were used, in order to simulate a normal heart, exercise activity, dilated cardiomyopathy, and hypertrophy. The variations between these different scenarios were the overall EF, wall thickness, cavity volume, and heart rate (HR). These parameters were tuned to closely match the relevant physiological differences between the simulated models, as shown in *Table 1*.

The deformation fields generated with the kinematical model were used to displace ultrasound scattering in the myocardium with realistic motion patterns, which were then used as an input to a custom ultrasound image simulation platform developed in-house (COLE, KU

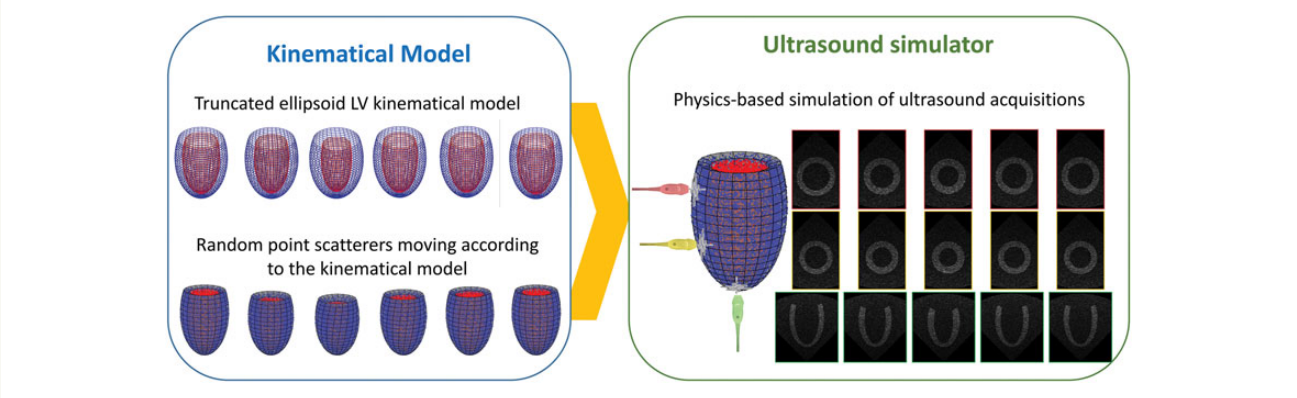

Figure 1 Diagram of the image simulation platform. A kinematic model is used to animate a cloud of point scatterers which move together with a contracting ellipsoidal LV model (left). Based on these points, an algorithm simulates the ultrasound wave propagation into the tissues and respective echoes arising from the point scatterers, which are then used to build the simulated image sequences.

Table 1 Reference values for global strains of the silico-simulated model

	Normal	Exercise	Hypertrophy	Dilated cardiomyopathy
Longitudinal				
Sub-endocardial strain (%)	−19.29	−24.18	−18.36	−9.38
Mid-myocardial strain (%)	−13.85	−17.10	−11.39	−7.52
Trans-myocardial strain (%)	−14.08	−17.45	−11.77	−7.56
Sub-epicardial strain (%)	−9.91	−12.13	−6.99	−5.98
Circumferential				
Sub-endocardial strain (%)	−29.30	−29.31	−29.31	−13.88
Mid-myocardial strain (%)	−16.44	−20.46	−12.16	−9.52
Trans-myocardial strain (%)	−17.32	−21.67	−13.63	−9.74
Sub-epicardial strain (%)	−10.34	−12.83	−6.35	−6.89
Radial				
Myocardial strain (%)	37.21	47.99	29.87	18.09

Leuven, Belgium).[17] At the core of this software tool lays an algorithm able to simulate the physical interactions between a propagating ultrasound wave and the point scatterers in the underlying tissue. This enables the modelling of the ultrasound image formation process, thus allowing creation of the corresponding ultrasound images associated with the aforementioned LV kinematical models. Furthermore, different acquisition parameters such as the FR, ultrasound line density, opening angle, and scan depth can be adapted to match a specific system. For the current study, the system was configured to mimic a generic 3 MHz cardiac probe generating images with an overall contrast-to-noise ratio of 8 dB (equivalent to 40% of noise in the blood pool). *Figure 2* and Supplementary data online, *Videos S1* and *S2* display an example of an image of the model of a normal heart in the apical and parasternal short-axis (SAX) view. For all models, several DICOM loops were generated at frame rates of 20, 35, 50, 75, 90, and 110 frames/s.

One observer (A.R.) analysed the four models at each of the six different frame rates repeatedly (14–15 times). The number of repeated analyses was chosen in order to gain sufficient power for comparing test accuracies for each model and frame rate. Each analysis contained a short-axis view for global radial and global circumferential strain and one apical view for longitudinal strain.

Patient inclusion and data acquisition

Seventy consecutive patients referred to echocardiography were included in the study and written informed consent was obtained. Exclusion criteria were presence of atrial fibrillation or grossly varying HR (changes in RR interval >20%). All echocardiographic studies were performed using an iE33-scanner (S5-1 probe, Philips Medical Systems, Andover, MA, USA) and a 1–5 MHz transducer with the patient in the left-lateral decubital position. Conventional 2D grey-scale images were obtained in the apical four-chamber views (4CH) and mid-ventricular SAX views. When long- or short-axis views displayed poor 2D quality, the views at all FR were either not acquired or excluded from later data analysis. Both views were repeatedly acquired at 3–6 differing FR with a range between 26 and 117 Hz. Highest FR was depending on image depth, width, and quality, while machine settings allowed no lower FR than 26 Hz. A single observer (A.R.) analysed all acquisitions once.

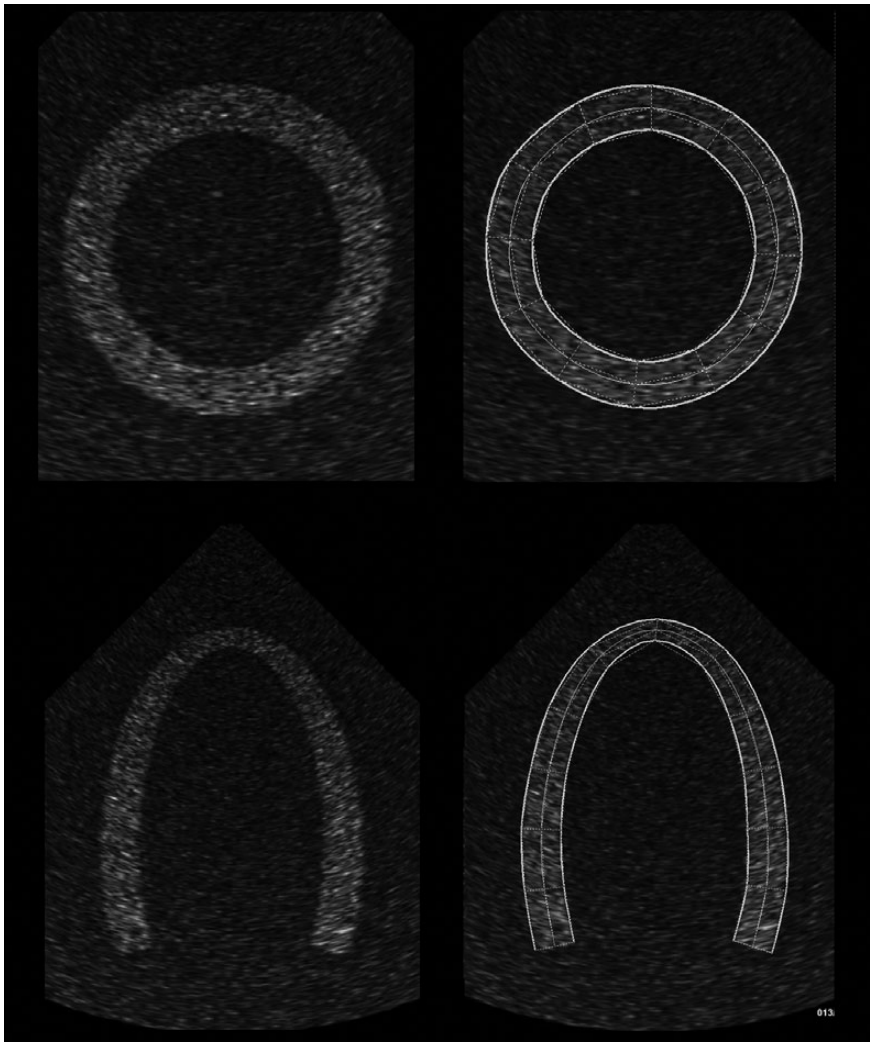

Figure 2 Original frame of the silico-simulated model in an apical and short-axis view to the left and the same model with tracking borders of the speckle-tracking software to the right.

Data processing

In the model and patients, strain analyses were performed with a 2D speckle-tracking software package (eSie® Velocity Vector Imaging, Siemens, Medical Solutions, Mountain View, CA, USA). *Figure 2* and Supplementary data online, *Videos S2* and *S4* demonstrate the tracking borders on a synthetic model. From the same tracking sequence, global strains were calculated for sub-endocardial (endo), myocardial (myo), and sub-epicardial (epi) measurements. Since the VVI software measures directly at the endo- and epicardial border, the region of interest was adapted to regionally varying muscle thickness. The ROI was manually drawn at the endo- and epicardial border of the first frame of a cardiac cycle. Tracking was a fully automated process, followed by visual assessment to validate if the tracked contours sufficiently matched myocardial borders throughout the cardiac cycle. If tracking was not approved, borders on the first frame were adjusted with consecutive new automated tracking. For longitudinal and circumferential strains, negative systolic peak values, and for radial strains, positive systolic peak values were extracted from the data set. In the simulated LV models, we chose to analyse peak strain values over the entire cardiac cycle. These represented systolic peaks since the kinematic model did not contain post-systolic strain (*Figure 3*). In patients, peak strains were measured during the ejection time (ET) period, which was defined by aortic valve opening and closure from Doppler measurements over the aortic valve.

Reproducibility

For intraobserver variability, the same observer (A.R.) reanalysed the same loops 3–4 weeks after the first analyses, while for interobserver variability, a second independent observer (E.A.) blinded for the data analysis of the first observer reanalysed the same loops. For inter- and intraobserver variabilities, the same 30 DICOM loops for short-axis and 30 DICOM loops for long-axis of the computed models were reanalysed. Furthermore, in the patient data set, 79 4CH and 75 SAX loops at differing frame rates were reanalysed by both observers. Intraclass correlation coefficients and Bland–Altman plots were derived from both the computed models and patient data. In order to estimate test–retest (i.e. inter-study) variability, the same models were re-generated resulting in images with different speckle patterns due to the random positioning of individual point scatterers in the simulation process. As such, new images with distinct speckles were generated as if it were new acquisitions. These new images were then also analysed by the same reader (D.K.).

Statistical analyses

All statistical analyses were performed using IBM SPSS Statistics 21 software (IBM Corporation, USA). For the synthetic data mean, standard deviation (SD) and confidence interval were calculated for the difference between the measured strain values and the given reference value of the model. Results in patient and synthetic data sets were grouped by FpC. In the synthetic data where references were values according to the model, ANOVA for dependent variables with Bonferroni adjusted analyses were used in order to identify differences between FpC groups. Coefficients of variation were calculated for repeated measurements. In the simulated models, the influence of several factors (i.e. FpC, endo-myo-epicardial ROI position, type of model, and peak strain values of the reference) on estimate-accuracies was analysed by univariable and multivariable regression analyses.

In assessment of the association between ET-strain with grouped FpC in patients, we used linear mixed models a statistical method combining regression analysis and repeated measurements. According to the results from simulated models, strain measurements at 46–65 FpC were set as reference for Bonferroni analysis in the mixed model for data derived from patients.

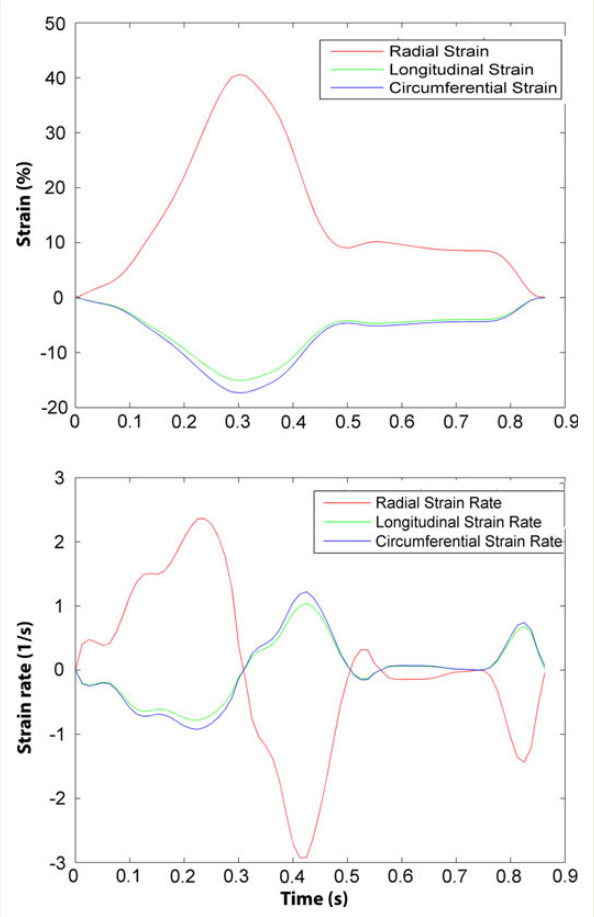

Figure 3 Example of strain and SR curves from the computed model (myocardium of the normal heart).

Results

Synthetic data

Table 1 shows reference values of the simulated models. *Table 2* and *Figure 4* show the difference between measured strain and the reference strain value for different FpC. A plateau for highest accuracies for strain measurements was achieved at >30 FpC for longitudinal and circumferential strains. *Table 2* and *Figure 4* show accurate estimates of longitudinal and circumferential strains. *Figure 4* demonstrates that the hypertrophy model slightly overestimated myocardial circumferential and longitudinal strain. According to *Table 2* and *Figure 4* in global radial strain, the plateau was reached at 50 and 40 FpC, respectively. In general, radial strain was underestimated. Compared with circumferential and longitudinal strain, both radial SD and CoV were significantly higher. The right column of *Figure 4* depicts the same results grouped by differing FRs. The right-shift of the exercise model demonstrates the influence of high HRs on measured strain values.

Table 3 shows univariable and multivariable regression analyses for the simulated models investigating possible factors influencing the

Table 2 Computed models: accuracy and variability of strain measurements in dependency of frame rates

Frames/Cardiac cycle	*n*	Mean (%)	± SD (%)	CI Lower bound (%)	CI Upper bound (%)	*P*-value (comparison to reference group)	Coefficient of variation (%)
Difference global peak systolic longitudinal strain							
8	42	13.2	3.5	12.1	14.3	<0.0001	6.3
14	84	4.8	3.1	4.1	5.4	<0.0001	4.5
15–20	129	3.5	1.2	3.3	3.7	<0.0001	4.9
25–30	171	0.9	0.8	0.8	1.0	<0.0001	4.2
31–40	84	0.2	0.9	−0.04	0.3	1.00	4.4
41–50	129	0.1	0.7	−0.1	0.2	1.00	5.0
51–65	129	−1.0	0.8	−1.2	−0.9	<0.0001	5.3
66–80	129	−0.5	0.9	−0.7	−0.3	0.063	7.0
81–95	129	−0.5	1.0	−0.7	−0.3	0.053	8.2
Difference global peak systolic circumferential strain							
8	42	17.5	8.4	14.9	20.1	<0.0001	5.8
14	84	7.1	6.5	5.7	8.5	<0.0001	5.0
15–20	129	5.1	4.2	4.4	5.9	<0.0001	4.9
25–30	171	2.1	2.5	1.7	2.5	0.181	2.8
31–40	84	2.0	2.9	1.4	2.6	1.00	4.9
41–50	129	0.9	2.2	0.5	1.3	1.00	3.9
51–65	129	0.6	1.5	0.3	0.8	1.00	4.0
66–80	129	0.6	1.5	0.3	0.8	1.00	3.5
81–95	129	0.8	1.5	0.5	1.1	1.00	4.1
Difference global peak systolic radial strain							
8	14	−42.0	0.8	−42.4	−41.6	<0.0001	12.5
14	28	−22.0	12.6	−26.8	−17.1	<0.0001	24.0
15–20	43	−18.1	6.4	−20.1	−16.2	<0.0001	11.6
25–30	57	−10.9	5.4	−12.4	−9.5	<0.0001	7.1
31–40	28	−10.6	8.9	−14.1	−7.1	0.001	12.3
41–50	43	−9.0	5.0	−10.5	−7.4	0.017	8.3
51–65	43	−4.2	2.8	−5.0	−3.3	1.00	9.8
66–80	43	−5.0	3.8	−6.2	−3.8	1.00	5.6
81–95	43	−4.1	4.1	−5.2	−2.7	1.00	9.1

Differences of measured Strain-reference Strain. Results of 14–15 times repeatedly measured endo-, myo-, and epicardial strains of the four different computed models at six frame rates between 20 and 110 Hz. Radial strains were expressed as one transmural measure. *P*-values express the comparison between the Frame per Cycle groups with lowest mean deviation from the reference. The differences of measured strains and reference values express test accuracies while the coefficient of variation reflects reproducibility for 14 repeated measurements at each frame rate. Confidence intervals derived from standard error of the mean (SEM).

accuracy of strain measurements in the *in-silico* models. A dependency of strain measurements on FR, model, and the strain magnitude in the circumferential direction was shown. Especially the DCM model displayed significantly lower strain variabilities and the exercise model higher strain variabilities. ROI position in the subendo-, myo-, or subepicardium showed higher variances in sub-endocardial positions compared with sub-epicardial ones in the univariable regression. This was probably caused by the difference in absolute strain values as shown in multivariable regression analyses where ROI had no effect on variabilities when corrected for strains.

Patient data

Of 70 patients, four were excluded due to atrial fibrillation. Seventeen SAX views and 11 apical views were discarded due to insufficient imaging quality. Of all patients included, 24 had systolic pathology including LV hypertrophy, ischaemic heart disease and heart failure, 22 patients had valvular or aortic diseases, three patients had diastolic heart failure, two right heart failure, three pericardial effusions, and 12 were assessed as normal. Ejection fraction was normal (>50%) in 55 patients, in eight patients EF was moderately reduced (35–50%), and in three patients EF was severely reduced (<35%).

Figure 5 and *Table 4* illustrate results from repeated measurements in patients at varying frame rates. Based on the results of the synthetic models, we chose the strain measured at 46–65 FpC as reference. A plateau was reached at strain values >25 FpC for circumferential and longitudinal strain, and >35 FpC for radial strain. For longitudinal strain measurements, at higher FpC than 85 a significant deviation

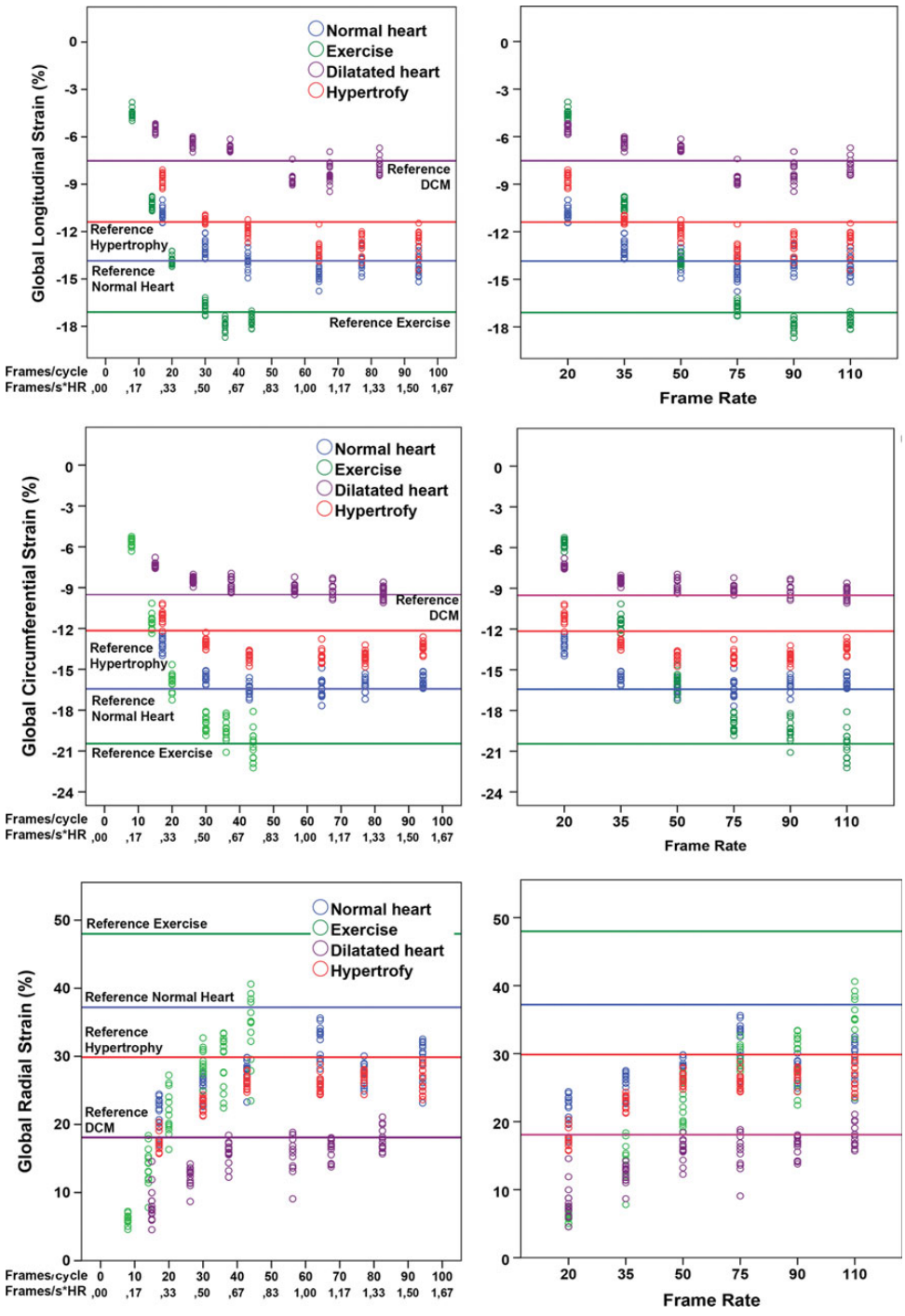

Figure 4 Mid-myocardial strain measures of four different models in three dimensions. The reference values are depicted as lines. Left column: correlation with frames per cycle (FpC). Right column: correlation with frames per second (Fps) without correction for high or lower HRs.

from the expected value was observed, while higher frame rates did not influence circumferential or radial strains significantly.

Reproducibility

Intra- and interobserver variabilities for synthetic and patient data are displayed in *Table 5* and as Bland–Altman plots in *Figures 6* and *7*. Significantly higher variabilities were observed in the patient data for longitudinal and circumferential strains with intraclass correlations from 86.1 to 97.6% compared with 98.4 to 99.4% in the synthetic data. Radial strains showed significantly higher variabilities for both synthetic data and patients.

Table 3 Univariable and multivariable regression for strains in computed models

Predictors	Univariable regression (Unadjusted model)					Multivariable regression (Adjusted final model)			
	Beta	95% CI	95% CI	*P*-value	R^2	Beta	95% CI	95% CI	*P*-value
Global peak systolic longitudinal strain									
Frames/cycle	−0.003	−0.003	−0.003	<0.0001	0.241	−0.003	−0.003	−0.002	<0.0001
Strain value	−0.001	−0.003	0.001	0.153	0.001				
Model									
Normal	Ref				0.129	Ref			<0.0001
Exercise	0.119	0.093	0.146	<0.0001		0.043	0.016	0.070	
DCM	−0.042	−0.069	−0.016	0.002		−0.042	−0.066	−0.018	
Hypertrophy	0.019	−0.007	0.046	0.156					
Location									
Endo	Ref				0.007				
Myo	−0.032	−0.06	0.007	0.011					
Epi	−0.034	−0.06	0.010	0.006					
						$R^2 = 0.268$			
Global peak systolic circumferential strain									
Frames/cycle	−0.004	−0.004	−0.003	<0.0001	0.324	−0.003	−0.003	−0.002	<0.0001
Strain value	−0.006	−0.007	−0.005	<0.0001	0.129	−0.004			<0.0001
Model									
Normal	Ref				0.252	Ref			<0.0001
Exercise	0.188	0.164	0.213	<0.0001		0.071	0.055	0.103	
DCM	−0.011	−0.035	0.014	0.389		−0.022	−0.043	−0.001	
Hypertrophy	0.005	−0.020	0.029	0.697					
Location									
Endo	Ref				0.036				
Myo	0.011	−0.013	0.035	0.355					
Epi	0.072	−0.048	0.096	<0.0001					
						$R^2 = 0.445$			

Beta is the standardized coefficient of the regression model.
CI, upper and lower confidence intervals.

Discussion

The major findings of the study showed that longitudinal and circumferential strain were correctly estimated at >30 FpC in synthetic data, while a plateau was reached in patients at >25 FpC. Both, in longitudinal and circumferential direction, sub-endocardial strains were significantly higher than sub-epicardial strains, without significant effect on estimate-accuracies. Radial strains were at all FpC underestimated and had significantly highest variabilities.

Accuracies in the synthetic data set

Speckle-tracking echocardiography strain measurements have previously been evaluated against MRI tagging or microcrystals.[18] However, MRI tagging also presents technical challenges that reduce overall accuracy. Microcrystals have limitations related to out of plane motion, in addition to mismatch problems arising from the non-trivial spatial association of reference values and STE measurements. The simulation platform in the present study was developed with the intention to make standardized evaluation of speckle-tracking software possible and to help improving machine settings and software.[19] Thus in the present study, it was possible to investigate reproducibility and accuracy at different frame rates with corresponding reference values in endo-, myo-, and epicardial position.

The simulated images had relatively low noise level, no artefacts, and easily detectable myocardial borders. The reference values were correctly detected in longitudinal and circumferential direction for FpC>30 corresponding to >50–60 Hz at normal (adult) HR. Accuracies of strain estimates in longitudinal and circumferential directions were high.

Strain-gradients through the myocardial wall have been described earlier.[20–23] However, strains have been calculated as 'layer' strains and not strains along the endo- or epicardial borders. With the VVI system, strains are being calculated in the endocardial borderline and epicardial borderline. Based on average patient data, *Figure 5* shows a four-fold higher endocardial circumferential and two-fold higher longitudinal strain in the endocardium compared with an epicardial ROI. In addition, hypertrophic geometry increases these endo-epicardial gradients as shown in *Table 1*. In order to make strain measurements, comparable correct position of the ROI and the clear specification of measurements are needed.[19]

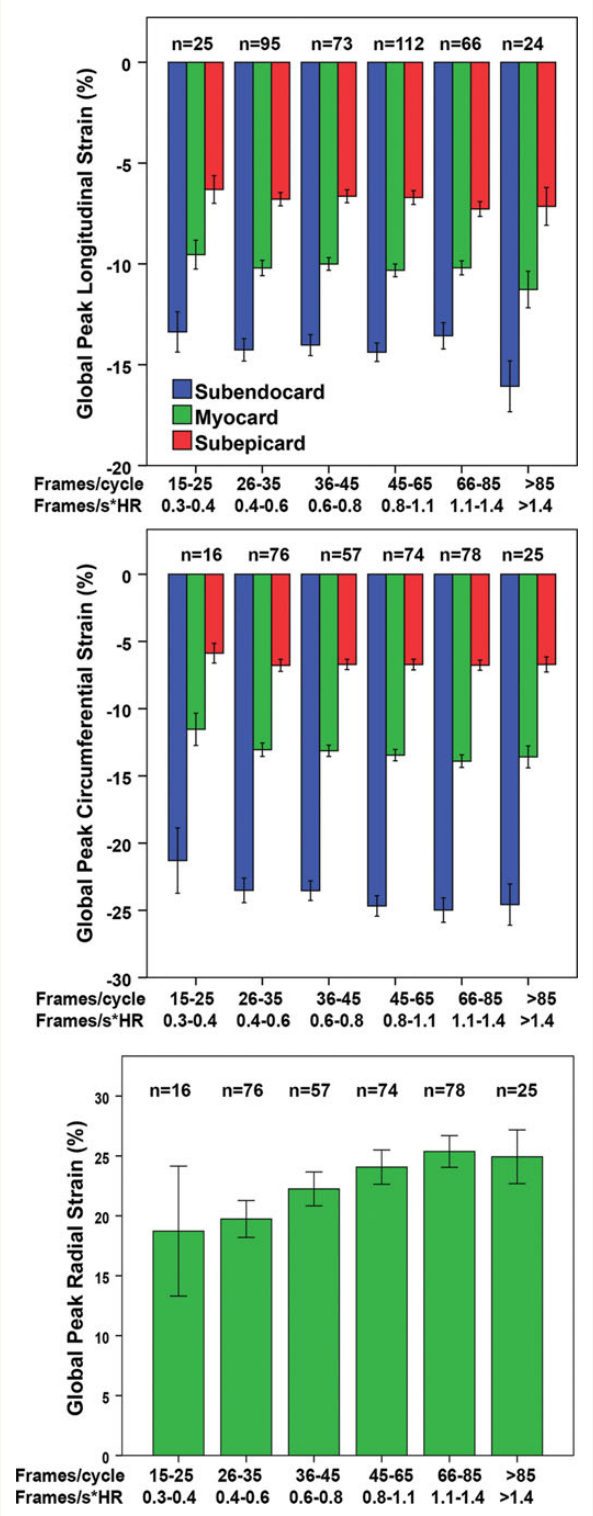

Figure 5 Mean endo-, myo-, and epicardial strains in dependency of frames per cycle (FpC) in patients. The confidence intervals are derived from intraindividual variations of repeated measurements at different frame rates.

Furthermore, much higher CoV differences between observers compared with intraobserver variability in patients, mirror the problem of non-uniform definition of the endo- and epicardial borders and the resulting high variabilities of strain estimates when these borders are differently defined. In computed models, where image quality was high and borders were easily detectable, intra- and interobserver variabilities were distinctly lowered. Thus, high image quality and a correct definition of myocardial borders seem to be crucial.

Table 4 Patient data: systolic strain measurements in dependency of frame rates

Frames/Cardiac cycle	*n*	Mean	± SD	*P*-value
Global peak systolic longitudinal strain (%)				
15–25	75	−7.6	4.7	0.058
26–35	284	−10.3	5.7	1.00
36–45	219	−9.6	5.5	1.00
46–65	336	−9.9	5.5	
66–85	198	−11.8	5.5	1.00
>85	72	−14.2	6.5	0.001
Global peak systolic circumferential strain (%)				
15–25	51	−12.8	8.0	<0.0001
26–35	231	−14.0	9.0	0.598
36–45	171	−13.5	8.3	0.934
46–65	225	−15.0	9.4	
66–85	237	−15.3	9.2	1.00
>85	78	−18.4	9.9	1.00
Global peak systolic radial strain (%)				
15–25	16	16.3	11.3	0.028
26–35	76	18.8	9.2	0.004
36–45	57	21.7	8.9	1.00
46–65	74	24.5	9.9	
66–85	78	25.2	10.2	1.00
>85	25	29.7	8.6	0.278

Results of endo-, myo-, and epicardial strains in 66 patients. One long-axis and one short-axis views were repeatedly acquired at 4–6 different frame rates. Mixed models analysis was performed with regard to repeated measurements on differing FpC groups and the mean strain value for each patient in subendo-, myo-, and sub-epicardial position. Measurements at 46–65 frames per cycle (FpC) were regarded as optimal and thus set as reference for comparison between FpC groups.

The influence of frame rate

Since time periods of cardiac events shorten at increasing HR, we chose to report our data as FR corrected for HR (FpC) rather than FR. Increasing FpC increased strain estimates until a plateau was reached (i.e. no significant change between reference value and estimate). Data from synthetic imaging confirmed the assumption that too low FpC leads to systematic underestimation of strain values. However, already >30 FpC rendered excellent strain accuracies for longitudinal and circumferential strains. In contrast to the previous publications on TVI-derived strain and frame rate,[11–13] the recommended frame rate of >100 Hz seems not to be needed for peak longitudinal circumferential or radial 2D-strains. Note, however, that TVI strains derived from STE are estimated through integration of strain rates derived from velocity differences. Underestimation of short lived SR peaks will thus lead to underestimation of TVI-derived strains. In STE, strain is derived from displacement of several points. Displacement curves contain less high-frequency

Table 5 Intra- and interobserver variabilities for strain- and SR measurements

Computed models	Intraclass correlation (% CI)		
	Longitudinal strain $n = 90$	Circumferential strain $n = 90$	Radial strain $n = 30$
Intraobserver variability (AR)	98.7 (98.1–99.2)	99.4 (99.1–99.6)	84.1 (66.5–92.4)
Interobserver variability (AR/EA)	98.4 (97.2–98.9)	99.1 (98.5–99.4)	72.6 (42.8–86.9)
Test–retest analysis in computed models	$n = 72$	$n = 72$	$n = 24$
Test variability (DK)	99.6 (99.4–99.8)	98.8 (98.0–99.3)	91.7 (80.8–96.4)
Retest variability (DK)[a]	98.4 (97.2–99.0)	98.7 (97.6–99.3)	90.4 (69.4–96.4)
Patients	$n = 201$	$n = 186$	$n = 66$
Intraobserver variability (AR)	94.9 (93.4–96.1)	97.6 (96.8–98.2)	82.8 (71.8–89.5)
Interobserver variaiblity (AR/EA)	86.1 (71.5–92.0)	94.0 (89.0–96.2)	80.7 (67.4–88.5)

[a]Test–retest analysis of two sets of simulated data with the same reference values.

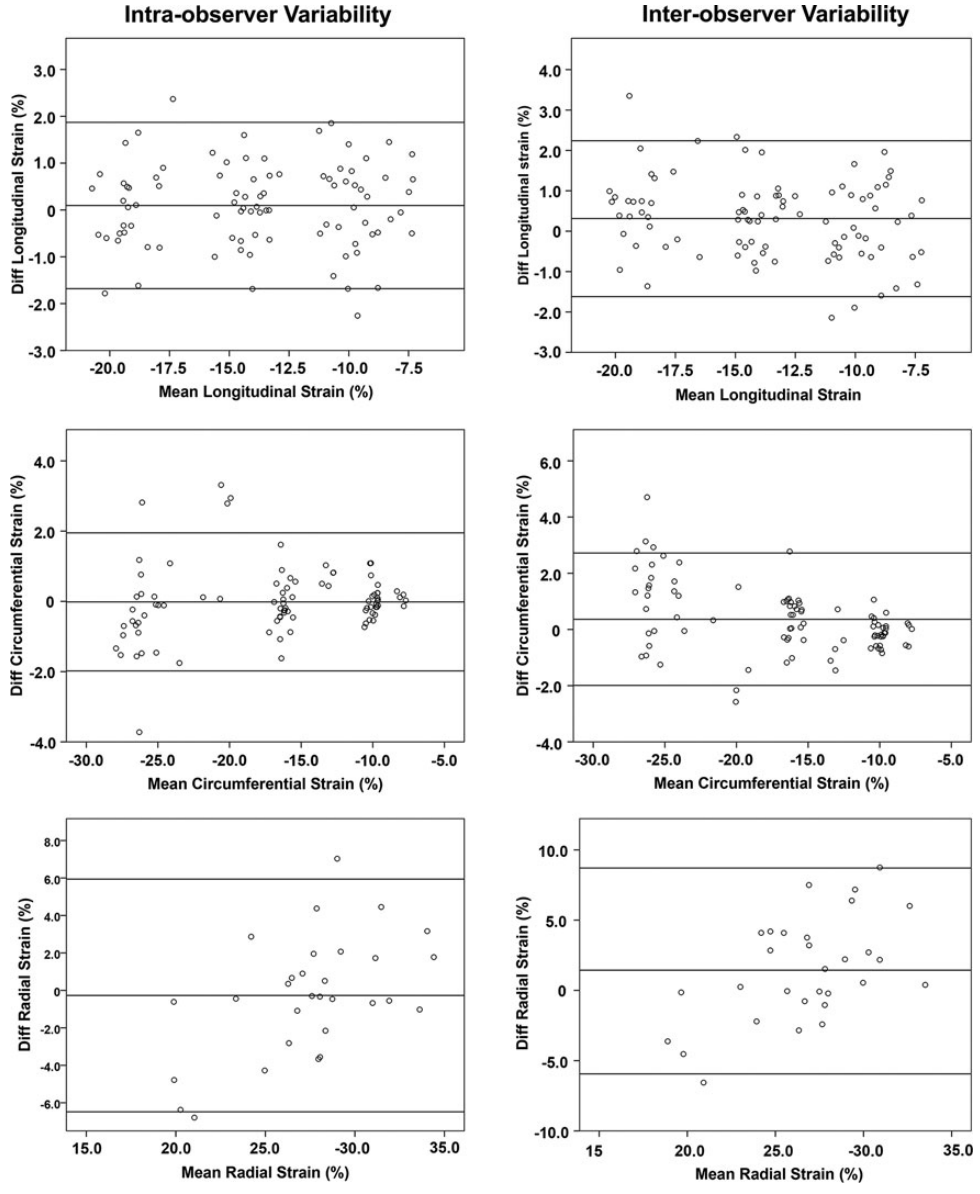

Figure 6 Intra- and interobservervariabilities as Bland–Altman plots in the silico-simulted models.

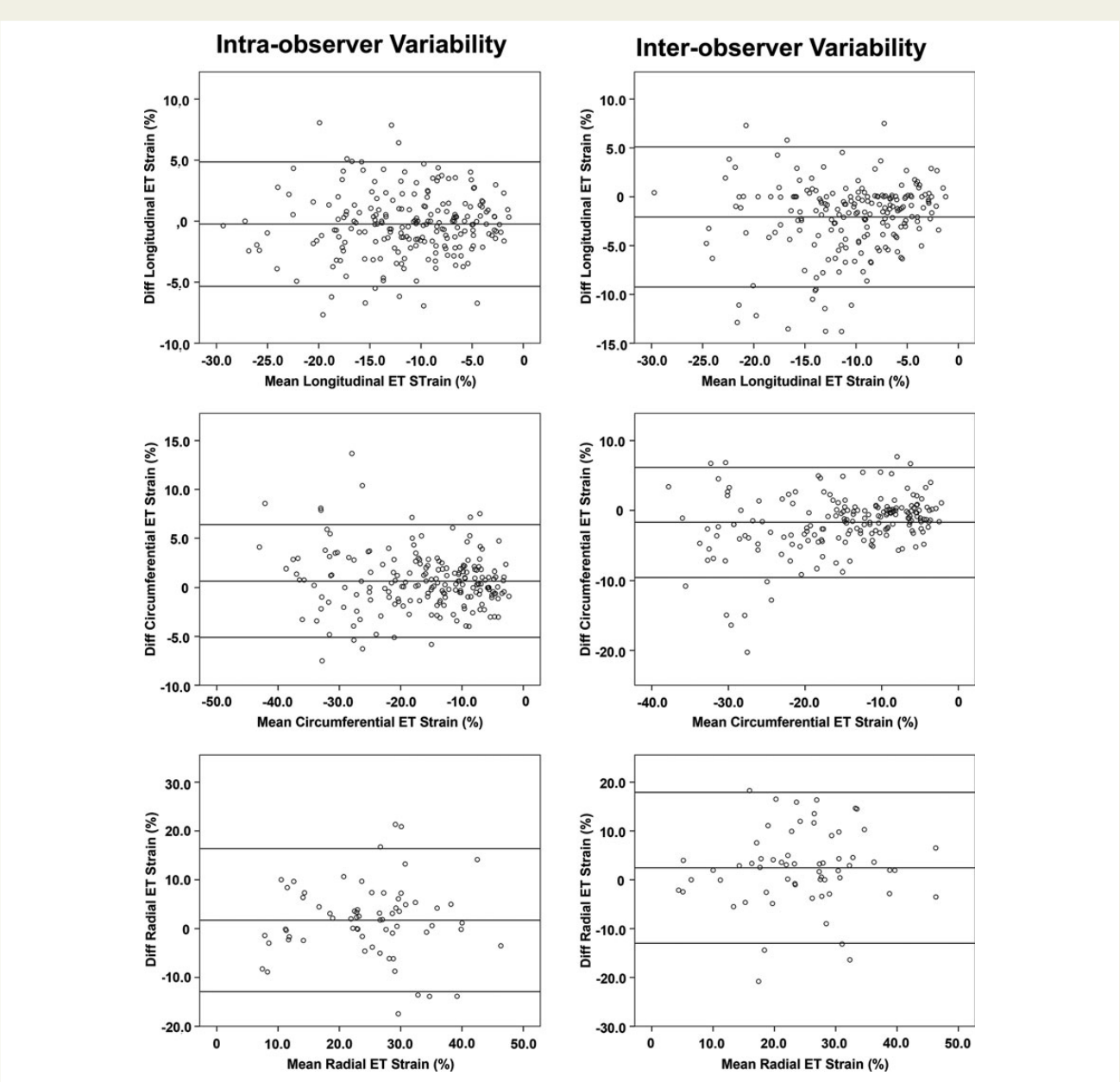

Figure 7 Intra- and interobserver variabilities as Bland–Altman plots in patients.

components (i.e. sudden changes), which allows a much lower frame rate for correct definition of broad peak strain values.

Only the highest FpC increased the variance of repeated measurements or strain accuracies. This indicates, that a FR-dependent tracking error accumulation does not occur at FpC <80. In all ultrasound systems, the trade-off between increasing FR and decreasing spatial resolution has to be made. Decreased spatial resolution would likely result in higher variabilities of measurements.

In a meta-analysis investigating normal GLS, frame rate had no impact on peak strain values.[14] Studies included in the analysis used optimized frame rates at the mid-range. Both synthetic and patient data of the present study demonstrate, that a wide range from 25 to 85 FpC rendered constant strain accuracies. Thus, it can be assumed that machine settings and average HRs of the meta-analysis studies render a majority of measurements within that range, thus being in concordance to our results.

The combination of high strains at high HR seems to be a challenge, since accuracy in the simulated exercise model was lower than in the normal heart case. However, in the synthetic model, imaging loops with >85 Fps allowed detection of the correct strain values at HR 160/min, while lower FR systematically underestimated strains. Thus, one has to be aware of the limitations of speckle-tracking algorithms when applying stress tests or high strains combined with high HR in infants or small animal studies, where machine settings are often below 85 Fps and HR higher than 160/min. These findings might be one factor explaining lower sensitivity and specificity of 2D strains compared with TVI strains in dobutamine stress echocardiography.[24]

Reproducibility of longitudinal, circumferential, and radial strain

In order to investigate primarily the effect of different frame rates on measured strain values, we chose to use a model with little noise resulting in much higher reproducibility compared with the echocardiographic data. In the patients, all data of one imaging view were either included or discarded due to poor imaging quality. No single segments were excluded from analysis. Thus, the patient data set included the normal range of regional echocardiographic artefacts, resulting in higher intra- and interobserver variabilities compared with synthetic data. Pathological curves with low and inverted systolic strain might also cause higher variation of peak systolic strain measurements. Accordingly, in the clinical setting, variabilities due to noise, inaccurate timing, and artefacts seem to outrange by far the influence of FpC.

In synthetic data, reproducibility and accuracy were very high for longitudinal and circumferential strains and lower for radial strains. In longitudinal and circumferential direction, global strain is measured along a line either anchored in the easily detectable structure of the mitral ring or in a closed cycle. Small tracking errors along the line get corrected by the software's algorithm keeping all points within a line. In contrast, erroneous definition of the endocardial border summate all errors of endo-epicardial distances for radial strain. Thus, the error of defining a too thick or too thin myocardium can be high in GRS, while GCS stays a robust measure in the same tacking sequence of an imaging loop.

Limitations

It should be emphasized that the current study focused on the estimates of peak systolic strain. Strain rate was not investigated since the model was not created for SR estimates. Correct timing is also dependent on high frame rates but has not been investigated in the current study. Incorrect timing of the ECG setting towards the first frame of the cardiac cycle might reduce peak strain values by wrong definition of end-diastole. The variability of strain estimates, especially in dependency on high frame rates is likely to be vendor or algorithm dependent. Therefore, it is unclear whether the results can be directly extrapolated to those obtained by other echocardiographic platforms.

Conclusion

Standard machine settings with a FR of 50–60 Hz allow correct peak global longitudinal and circumferential strain at normal (adult) HR and imaging at >30 FpC may be adequate for assessment of GCS and GLS, while the quantification of radial strain cannot be recommended for clinical use yet. The influence of correct definition of the region of interest within the myocardium seems to be of highest importance for accurate 2D peak strain estimation.

Supplementary data

Supplementary data are available at *European Heart Journal – Cardiovascular Imaging* online.

Conflict of interest: None declared.

References

1. Sjoli B, Grenne B, Smiseth OA, Edvardsen T, Brunvand H. The advantage of global strain compared to left ventricular ejection fraction to predict outcome after acute myocardial infarction. *Echocardiography* 2011;**28**:556–63.
2. Aarsaether E, Rosner A, Straumbotn E, Busund R. Peak longitudinal strain most accurately reflects myocardial segmental viability following acute myocardial infarction - an experimental study in open-chest pigs. *Cardiovasc Ultrasound* 2012; **10**:23.
3. Hanekom L, Jenkins C, Jeffries L, Case C, Mundy J, Hawley C *et al.* Incremental value of strain rate analysis as an adjunct to wall-motion scoring for assessment of myocardial viability by dobutamine echocardiography: a follow-up study after revascularization. *Circulation* 2005;**112**:3892–900.
4. Ingul BC, Rozis E, Slordahl SA, Marwick TH. Incremental value of strain rate imaging to wall motion analysis for prediction of outcome in patients undergoing dobutamine stress echocardiography. *Circulation* 2007;**115**:1252–9.
5. Ternacle J, Berry M, Alonso E, Kloeckner M, Couetil JP, Rande JL *et al.* Incremental value of global longitudinal strain for predicting early outcome after cardiac surgery. *Eur Heart J Cardiovasc Imaging* 2013;**14**:77–84.
6. Magne J, Mahjoub H, Dulgheru R, Pibarot P, Pierard LA, Lancellotti P. Left ventricular contractile reserve in asymptomatic primary mitral regurgitation. *Eur Heart J* 2013; **35**:1608–16.
7. Ersboll M, Valeur N, Mogensen UM, Andersen MJ, Moller JE, Velazquez EJ *et al.* Prediction of all-cause mortality and heart failure admissions from global left ventricular longitudinal strain in patients with acute myocardial infarction and preserved left ventricular ejection fraction. *J Am Coll Cardiol* 2013;**61**:2365–73.
8. Amundsen BH, Helle-Valle T, Edvardsen T, Torp H, Crosby J, Lyseggen E *et al.* Noninvasive myocardial strain measurement by speckle tracking echocardiography: validation against sonomicrometry and tagged magnetic resonance imaging. *J Am Coll Cardiol* 2006;**47**:789–93.
9. Leitman M, Lysyansky P, Sidenko S, Shir V, Peleg E, Binenbaum M *et al.* Two-dimensional strain-a novel software for real-time quantitative echocardiographic assessment of myocardial function. *J Am Soc Echocardiogr* 2004;**17**:1021–9.
10. Ha JS, Walker WF, Hossack JA. Determination of an optimal image frame interval for frame-to-frame ultrasound image motion tracking. *IEEE Trans Ultrason Ferroelectr Freq Control* 2005;**52**:386–96.
11. Gunnes S, Storaa C, Lind B, Nowak J, Brodin LA. Analysis of the effect of temporal filtering in myocardial tissue velocity imaging. *J Am Soc Echocardiogr* 2004;**17**: 1138–45.
12. Lind B, Nowak J, Dorph J, van der Linden J, Brodin LA. Analysis of temporal requirements for myocardial tissue velocity imaging. *Eur J Echocardiogr* 2002;**3**:214–9.
13. Storaa C, Lind B, Brodin LA. Distribution of left ventricular longitudinal peak systolic strain and impact of low frame rate. *Ultrasound Med Bio* 2004;**30**:1049–55.
14. Yingchoncharoen T, Agarwal S, Popovic ZB, Marwick TH. Normal ranges of left ventricular strain: a meta-analysis. *J Am Soc Echocardiogr* 2013;**26**:185–91.
15. Arts T, Hunter WC, Douglas A, Muijtjens AM, Reneman RS. Description of the deformation of the left ventricle by a kinematic model. *J Biomech* 1992;**25**:1119–27.
16. Waks E, Prince J, Douglas A. *Cardiac motion simulator for tagged MRI*. Mathematical Methods in Biomedical Image Analysis 1996;182–91.
17. Gao H, Choi HF, Claus P, Boonen S, Jaecques S, Van Lenthe GH *et al.* A fast convolution-based methodology to simulate 2-D/3-D cardiac ultrasound images. *IEEE Trans Ultrason Ferroelectr Freq Control* 2009;**56**:404–9.
18. Amundsen BH, Crosby J, Steen PA, Torp H, Slordahl SA, Stoylen A. Regional myocardial long-axis strain and strain rate measured by different tissue Doppler and speckle tracking echocardiography methods: a comparison with tagged magnetic resonance imaging. *Eur J Echocardiogr* 2009;**10**:229–37.
19. Thomas JD, Badano LP. EACVI-ASE-industry initiative to standardize deformation imaging: a brief update from the co-chairs. *Eur Heart J Cardiovasc Imaging* 2013;**14**: 1039–40.
20. Ishizu T, Seo Y, Enomoto Y, Sugimori H, Yamamoto M, Machino T. Experimental validation of left ventricular transmural strain gradient with echocardiographic two-dimensional speckle tracking imaging. *Eur J Echocardiogr* 2010;**11**:377–85.
21. Rosner A, How OJ, Aarsaether E, Stenberg TA, Andreasen T, Kondratiev TV *et al.* High resolution speckle tracking dobutamine stress echocardiography reveals heterogeneous responses in different myocardial layers: implication for viability assessments. *J Am Soc Echocardiogr* 2010;**23**:439–47.
22. Matre K, Moen CA, Fannelop T, Dahle GO, Grong K. Multilayer radial systolic strain can identify subendocardial ischemia: an experimental tissue Doppler imaging study of the porcine left ventricular wall. *EurJ Echocardiogr* 2007;**8**:420–30.
23. Sarvari SI, Haugaa KH, Zahid W, Bendz B, Aakhus S, Aaberge L *et al.* Layer-specific quantification of myocardial deformation by strain echocardiography may reveal significant CAD in patients with non-ST-segment elevation acute coronary syndrome. *JACC Cardiovasc Imaging* 2013;**6**:535–44.
24. Hanekom L, Cho GY, Leano R, Jeffriess L, Marwick TH. Comparison of two-dimensional speckle and tissue Doppler strain measurement during dobutamine stress echocardiography: an angiographic correlation. *Eur Heart J* 2007;**28**:1765–72.